Spectroscopic and Theoretical Studies of Metal Cluster Complexes. 1. The He(I) Photoelectron Spectrum of Re_3Cl_9. Calculations by the SCC DV Xα Method of Re_3Cl_9 and $Re_2Cl_8^{2-}$

William C. Trogler,*[1a] Donald E. Ellis,[1a] and Joseph Berkowitz[1b]

Contribution from the Departments of Chemistry and Physics, Northwestern University, Evanston, Illinois 60201, and the Physics Division, Argonne National Laboratory, Argonne, Illinois 60439. *Received March 26, 1979*

Abstract: The gas-phase photoelectron spectrum of Re_3Cl_9 has been measured at ca. 800 K. The first vertical ionization potential occurs at 8.85 eV Results of a discrete variational Hartree–Fock–Slater calculation suggest that this ionization be attributed to a $^2E''$ state. Spin–orbit splitting of the first ionization band also supports this assignment. Charge density contributions to this orbital are distributed over the Re 5d, bridging Cl 3p, and axial Cl 3p orbitals in a 5:2:3 ratio. Remaining features in the photoelectron spectrum and the proposed orbital assignments are as follows: 9.80 eV, $22e''$; 9.90 eV, $18a_2''$, $12a_2'$, $40e'$; 10.47 eV, $21e''$; 10.83 eV, $39e'$, $17a_2''$, $5a_1''$; 11.09 eV, $28a_1'$, $20e''$, $38e'$; 11.83 eV, $16a_2''$, $37e'$; 12.21 eV, $11a_2'$, $36e'$; 13.06 eV, $27a_1'$; 13.39 eV, $15a_2''$, $19e''$, $26a_1'$; 13.86 eV, $35e'$. A unique feature of bonding in this complex is the great stability of $25a_1'$, the cluster σ-bonding orbital. Chemically, this manifests itself in a trans effect at the vertices of the trinuclear cluster framework. To allow a fair comparison between Re_3Cl_9 and the well-studied $Re_2Cl_8^{2-}$ ion, a calculation of the latter complex's electronic structure was also performed. A detailed comparison of the valence orbitals in these two molecules follows.

Introduction

Transition-metal cluster complexes offer a logical connection between the realms of coordination and solid-state chemistry. The possible similarity between chemical transformations which occur on metal surfaces and those which take place within the first coordination sphere of a metal cluster complex has been discussed.[2a] In some cases metal-surface-like catalytic activity has even been achieved with trinuclear transition metal cluster complexes under apparently homogeneous conditions.[2b] An understanding of the optical, electrical, and other physical properties of polymeric inorganic materials may also be enriched through a study of metal cluster complexes of increasing size. On a more fundamental level, these species provide discrete, well-defined situations for studying the nature of the metal–metal bond.

An insight into metal–metal interactions in binuclear complexes has been achieved owing to the efforts of many investigators.[3] To summarize, it has been found that some spectroscopic properties can be accounted for within a two-site coupling model. For some molecules an exchange or a weak coupling model seems appropriate. In other instances strong covalent bonding must be explicitly treated. Trinuclear metal cluster complexes also pose intriguing questions related to three-center delocalization. Eventually, we would like to correlate delocalized bonding properties of metal cluster complexes with their chemical reactivity. Certainly electronic structural studies of π-delocalized organic systems (i.e., the aromatics) have led to a better understanding of their reactions. We chose to initiate our study with Re_3Cl_9 (Figure 1) because chemical–structural[4] as well as vibrational spectroscopic[5] evidence point toward strong and direct metal–metal interactions. Furthermore, it is possible to examine this molecule in the gas phase, where it is isolated from environmental perturbations. Finally, because the $Re_2Cl_8^{2-}$ ion is frequently regarded as the prototypical metal–metal bond,[3] a study of the chemically related Re_3Cl_9 complex offered the possibility for some interesting comparisons.

Experimental Section

The cylindrical-mirror electron energy analyzer has been described previously.[6] A hollow-cathode lamp of the Newburgh type[7] served as the radiation source. Electrons were detected by a channeltron and after amplification the signal was stored in a multichannel analyzer and subsequently transferred to magnetic tape for computer analysis. Energy calibration was accomplished by recording spectra with Ar and He present. The $^2P_{3/2}$ IP of argon occurs at 15.7597 eV.[8] In the low-energy region we use the first IP of He (24.5869 eV)[8] which results from He(II) radiation emitted by the Newburgh lamp. About 10% of this lamp's output (in the vacuum UV) occurs at 304 Å (He(II)) and the remainder at 584 Å (He(I)). In the He(I) PES the ionization of He by He(II) radiation corresponds to a peak with an apparent ionization energy of 4.9913 eV. Spectral resolution varied between 50 and 100 mV as the sample deposited on surfaces near the ionization region. Small energy shifts also occurred, and therefore the uncertainty in peak positions is rather large (±0.05 eV).

Nonachlorotrirhenium(III) was purchased from Alfa-Ventron and purified by sublimation prior to use. The compound was loaded into a resistively heated platinum oven under a stream of argon and the entire apparatus was pumped down to 10^{-6} Torr before initiating sample heating. The He(I) photoelectron spectrum was continuously monitored and the oven gradually heated. At 500–600 K an increase in pressure was noted and the spectrum of a species, not Re_3Cl_9, was observed. A similar volatile impurity was noted in earlier mass spectral studies[9] and attributed to oxyhalides of rhenium. If the analyzer is removed at this point no appreciable deposits of dark-red Re_3Cl_9 are found on surfaces near the ionization region. If heating is continued, eventually the spectrum due to the spurious species disappears and further warming to ca. 800 K yields the Re_3Cl_9 vapor spectrum shown in Figure 2. Now, large quantities of solid Re_3Cl_9 are found deposited near the ionization region. We have reproduced the PES spectrum of Re_3Cl_9 on different occasions and employing different samples.

Electronic structure calculations were of the discrete variational[10] (DV) Xα type. The molecular electron density was approximated with an s-wave expansion (overlapping spherical functions on every center) in calculating the potential, and the SCF equations were converged by a self-consistent charge (SCC) procedure.[10] Numerical atomic orbitals were employed as basis functions. For Re all orbitals through 6p were included and for Cl those functions through 3p were used. Core orbitals were explicitly treated in these calculations. A transition state calculation was performed for the $^2E''$ state (ionization from the highest occupied 23 e'' orbital) and the remaining IPs in Table I were computed assuming similar relaxation as in the $^2E''$ state. Our experience[11] with systems such as $Mo(CO)_6$ indicates that this procedure will approximate the IPs within ±0.2 eV of the actual transition-state values. This result follows from the fact that the transition-state Hamiltonians for states with similar spatial character (i.e., valence orbitals) are comparable.

For the geometry of Re_3Cl_9, D_{3h} symmetry was assumed and bond

0002-7863/79/1501-5896\$01.00/0

Table I. Ionization Potentials in Re_3Cl_9. Experiment and Theory

IP (band max, eV)	orbital assigned to IP	calcd energy[a]
9.00, 8.85	$23e''$	8.7
9.80 (sh)[b]	$22e''$	9.7
9.90	$18a_2''$,$12a_2'$,$40e'$	9.8
10.47	$21e''$	10.2
10.83	$39e'$,$17a_2''$,$5a_1''$	10.5, 10.6, 10.9
11.09	$28a_1'$,$20e''$,$38e'$	11.2, 11.3, 11.3
11.83	$16a_2''$,$37e'$	11.9, 12.1
12.21 (sh)	$11a_2'$,$36e'$	12.5, 12.6
13.06	$27a_1'$	13.1
13.39	$15a_2''$,$19e''$,$26a_1'$	13.5, 13.6, 13.8
13.86	$35e'$	14.2

[a] The transition-state calculation was explicitly carried out for ionization from $23e''$. Remaining IPs were calculated assuming the same relaxation as was found for this level. [b] sh denotes a shoulder.

lengths and angles were averaged from the structure reported for $Cs_3Re_3Cl_{12}$,[12] except that the three terminal Cl^- ions in the Re_3 plane were removed. This assumption seems reasonable in view of the kinetic lability and long Re-Cl bond lengths for these three ions. Furthermore, the remaining Re_3Cl_9 framework persists structurally intact in a variety of $Re_3Cl_9L_3$ complexes.[12] Using Cl_b to denote the three bridging atoms in the Re_3Cl_9 structure, the bond lengths (in ångstroms) assumed were Re-Re (2.477), Re-Cl (2.359), Re-Cl_b (2.39), and bond angles (decimal degrees) were Re-Cl_b-Re (62.4), Cl-Re-Cl (157.8), Cl-Re-Cl_b (89.9), Re-Re-Cl_b (58.8). The exchange parameter α was taken to be 0.70 in all calculations. In the $Re_2Cl_8^{2-}$ calculation the atomic locations previously used[13] were employed.

Results and Discussion

The He(I) photoelectron spectrum of Re_3Cl_9 vapor at ca. 800 K is shown in Figure 2. Valence band ionizations are clustered between 8.5 and 14.5 eV. A distinct peak at 8.85 eV defines the vertical energy for the first IP. Energies of other band maxima and unresolved shoulders in the spectrum are also found in Table I. Previous mass spectral studies yielded a value of 10.5 eV[9] (by electron impact) for the appearance potential of $Re_3Cl_9^+$. From the spectrum in Figure 2 we find that the photoionization threshold occurs at much lower energy (ca. 8.6 eV). Specific assignments of these spectral features will follow the theoretical discussion.

Electronic structure calculations of quadruply metal-metal bonded binuclear systems have employed extended Hückel,[13,14] muffin tin Xα,[15] overlapping spheres or SCF Xα SW,[16] discrete variational (DV) Xα,[17] Hartree-Fock (with and without CI),[18] and generalized valence bond (GVB) methods.[19] A pseudopotential has been used to approximate core electron behavior in the latter two procedures. Of all these methods the Xα, HF-CI, and GVB treatments have proved most accurate. In the study of metal cluster complexes we have adopted the SCC DV Xα procedure for several reasons: (1) For three, four and six metal atom systems HF-CI and GVB calculations would, at present, be too demanding computationally. (2) The DV method incorporates no adjustable parameters, beyond α, which we always set equal to 0.70. (3) Because the DV approach is a numerical method, tabulated numerical atomic orbitals (NAOs) can be used as basis functions. Therefore, wave functions can be decomposed into atomic orbital contributions in the spirit of SCF-LCAO-MO calculations. This feature facilitates the analysis of intricate delocalized eigenfunctions. (4) The Xα "transition state" further provides a prediction of spectroscopic observables and permits a quantitative test of theory.

Results from a charge-density analysis of occupied valence band orbitals are given for the Re_3Cl_9 ground electronic state, within the SCC DV Xα method, in Table II. Ground-state orbital energies are also presented in this table. Ionization energies calculated by the transition-state procedure (Experimental Section) have been listed in column 3 of Table I. The NAO contribution to the charge density of the jth eigenvector in a specific symmetry block is defined[10] as

$$Q_j = q_{jj} + \sum_{k \neq j} \frac{q_{jj}}{(q_{jj} + q_{kk})} q_{jk}$$

where q_{jk} are entries in the appropriate charge-density matrix.

Table II. Charge Density Analysis of Occupied Valence Band Orbitals in the Re_3Cl_9 Ground State

orbital	eigenvalue, eV	major atomic orbital contributions[a] (% contribution)
$25a_1'$	−14.27	Re 5d (80) Re 6s (11) Re 5p (4)
$35e'$	−12.08	Re 5d (44) Cl_b 3p (46) Cl_b 3s (4)
$26a_1'$	−11.70	Re 5d (21) Cl_b 3s (8) Cl_b 3p (63)
$19e''$	−11.46	Re 5d (42) Cl_b 3p (37) Cl 3p (19)
$15a_2''$	−11.39	Re 5d (72) Cl 3p (22)
$27a_1'$	−10.98	Re 5d (14) Cl 3s (7) Cl 3p (66)
$36e'$	−10.49	Re 5d (22) Cl 3p (65) Cl 3s (8)
$11a_2'$	−10.36	Re 5 and 6p (4) Cl_b 3p (84) Cl 3p (5)
$37e'$	−10.02	Re 5d (3) Cl_b 3p (80) Cl 3p (9)
$16a_2''$	−9.80	Cl_b 3p (60) Cl 3p (33)
$38e'$	−9.22	Re 5d (62) Cl_b 3p (21) Cl 3p (13)
$20e''$	−9.17	Re 5d (17) Cl 3p (75)
$28a_1'$	−9.15	Cl 3p (95)
$5a_1''$	−8.82	Re 5d (33) Cl 3p (67)
$17a_2''$	−8.51	Cl_b 3p (33) Cl 3p (63)
$39e'$	−8.43	Re 5d (8) Cl_b 3p (20) Cl 3p (70)
$21e''$	−8.06	Cl_b 3p (35) Cl 3p (64)
$40e'$	−7.70	Re 5d (6) Cl 3s (8) Cl 3p (80)
$12a_2'$	−7.69	Cl_b 3p (9) Cl 3p (90)
$18a_2''$	−7.68	Re 5d (27) Cl 3p (67)
$22e''$	−7.61	Re 5d (6) Cl_b 3p (5) Cl 3p (87)
$23e''$	−6.55	Re 5d (50) Cl_b 3p (20) Cl 3p (30)

[a] The bridging chloride is denoted by the subscript b.

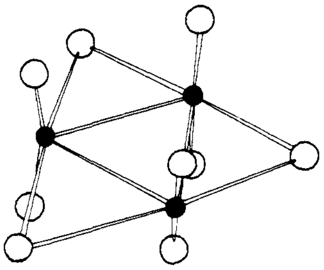

Figure 1. Structure of the Re_3Cl_9 moiety, where the solid circles denote rhenium atoms.

Both the calculated and experimental data show a cluster of IPs between ca. 9 and 14 eV. For the first vertical IP excellent correspondence exists between the spectroscopic measurement and that predicted by theory. Furthermore, there is excellent agreement between experiment and theory on the ca. 1 eV gap between the first and second IPs. Consistently (in three different spectra) splitting in the 9-eV band into components at about 9.0 and 8.85 eV is seen. This may be attributed to splitting of the $^2E''$ state into $E_{1/2}$ and $E_{3/2}$ spin-orbit components. We note that spin-orbit splitting of $^2E''$ states have been observed in the PES of MX_3 complexes[20] (M = B, Al, Ga, In; X = Br, I). In the present case it seems likely that the substantial heavy-atom Re d character of the $23e''$ orbital causes this effect. Further calculations are underway to incorporate relativistic corrections and explicitly treat multiplet splittings in both the photoionization and optical spectra.

The spectral region between 9.5 and 10.5 eV evidences considerable unresolved structure resulting from the cluster of orbitals $22e''$, $18a_2''$, $12a_2'$, $40e'$, and $21e''$, which are pre-

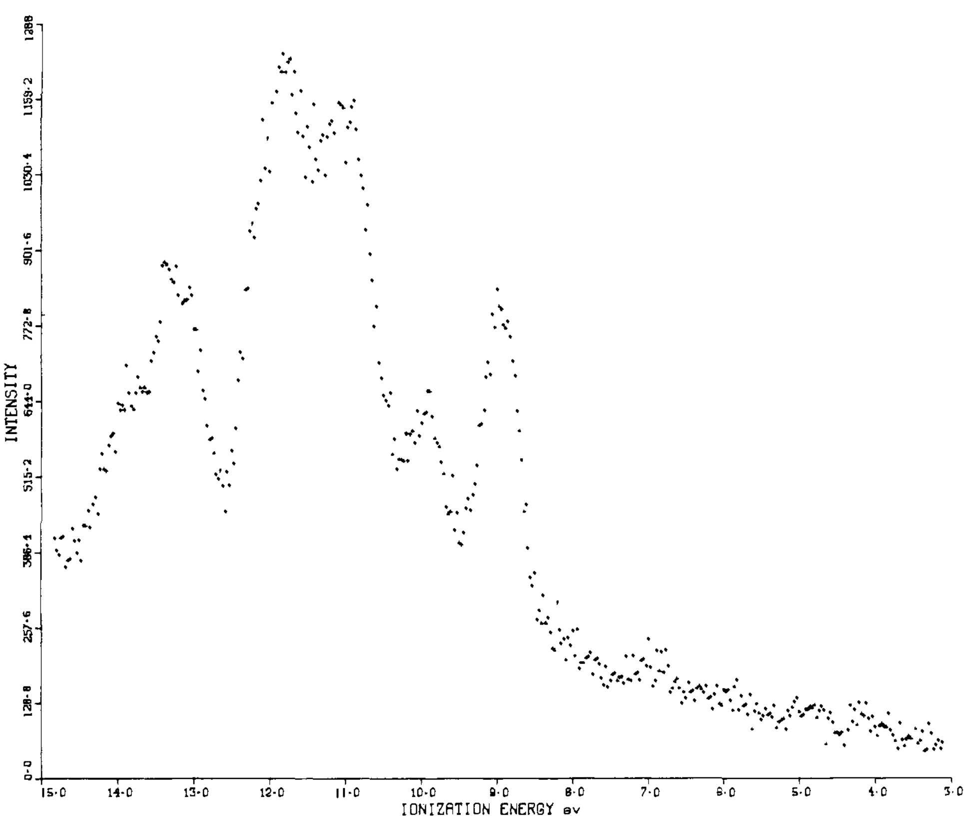

Figure 2. He(I) photoelectron spectrum of Re_3Cl_9 in the vapor phase at ca. 800 K.

Table III. Charge Density Analysis of Occupied Valence Band Orbitals in the $Re_2Cl_8^{2-}$ Ground State

orbital	eigenvalue,[a] eV	atomic orbital contributions (% contribution)
$9b_{1g}$	−11.57	Re 5d (30) Cl 3p (70)
$18a_{1g}$	−11.52	Re 5d (31) Cl 3p (63)
$15e_u$	−11.46	Re 5d (51) Cl 3p (47)
$5b_{2g}$	−11.46	Re 5d (27) Cl 3p (73)
$9b_{2u}$	−11.11	Re 5d (27) Cl 3p (73)
$5b_{1u}$	−10.89	Re 5d (20) Cl 3p (80)
$18a_{2u}$	−10.82	Re 5d (6) Re 6s (4) Cl 3s (3) Cl 3p (86)
$19a_{1g}$	−10.48	Re 5d (16) Cl 3p (75)
$15e_g$	−10.15	Re 5d (9) Cl 3p (86)
$16e_u$	−9.90	Cl 3p (94)
$20a_{1g}$	−9.54	Re 5d (41) Re 5p and 6p (9) Cl 3p (44)
$19a_{2u}$	−9.19	Re 5d (5) Cl 3p (91)
$10b_{1g}$	−9.04	Cl 3p (99)
$17e_u$	−8.81	Re 5d (5) Cl 3p (94)
$16e_g$	−8.56	Cl 3p (98)
$17e_g$	−8.50	Re 5d (4) Cl 3p (96)
$10b_{2u}$	−7.97	Cl 3p (100)
$2a_{2g}$	−7.96	Cl 3p (100)
$2a_{1u}$	−7.79	Cl 3p (100)
$18e_u$	−7.55	Re 5d (47) Cl 3p (50)
$6b_{2g}$	−6.41	Re 5d (82) Cl 3p (18)

[a] The eigenvalues have been uniformly shifted so that the shallow metal core levels in $Re_2Cl_8^{2-}$ match those in Re_3Cl_9.

dicted to have IPs in this energy region. An intense broad band system between 10.5 and 12.5 eV is split into major components at 10.9 and 11.8 eV. Plausible assignments are provided in Table I where we have maintained the relative ordering and clustering of levels predicted theoretically. After a minimum in the spectrum a broad structured band is found in the 13–15-eV region which is composed of 27a′ through 35e′ ionizations. In no case do we have to assume that calculated energies err by more than 0.4 eV; however, one cannot honestly expect this level of calculation to be precise within ±1.0 eV. When relativistic effects are incorporated, level shifts and some reordering may occur; however, the present calculation provides a reasonable account of the salient features in the ionization spectrum.

Although the calculation provides a reasonable assignment of *energies* in the photoelectron spectrum, there are some features which we do not fully understand. The relative band intensities do not appear to compare directly with the density of the occupied levels. In particular, the cross section for the first ionization appears unusually large, relatively speaking. There are some calculations[21] which suggest comparable cross sections for atomic Re 5d and Cl 3p ionizations at 21.2 eV of photon energy. Since, at the present time, no reliable theory exists for comparing atomic cross sections and those derived from extensively delocalized MOs, we merely note that a simple density of states argument does not appear valid.

Bonding interactions in Re_3Cl_9 differ significantly from those in the well-studied $Re_2Cl_8^{2-}$ ion. In both complexes the rhenium atom exists in a formal 3+ oxidation state. Previously, a muffin tin Xα calculation was reported for $Re_2Cl_8^{2-}$ using a frozen core approximation.[15] In order to directly compare NAO contributions for Re_3Cl_9 and $Re_2Cl_8^{2-}$ we have calculated the ground electronic state of the latter complex by the SCC DV Xα method. Core electrons were explicitly treated in this calculation and results are listed in Table III. Except for the placement of $9b_{2u}$ the orbital energy orderings are in close accord with the previous study.[15]

Let us now summarize the nature of the valence orbitals in $Re_2Cl_8^{2-}$ and Re_3Cl_9. Essentially pure Cl 3s levels ($17a_{1g}$, $17a_{2u}$, $8b_{1g}$, $14e_u$, $8b_{2u}$, and $14e_g$) lie between −21.37 and −20.537 eV in $Re_2Cl_8^{2-}$. This was earlier[16] found to be true for $Mo_2Cl_8^{4-}$ and evidences the small s-p mixing among chlorine valence orbitals. In Re_3Cl_9 the 23a₁′, 33e′, 24a₁′, 14a₂″, 34e′, and 18e″ orbitals, which lie between −22.18 and

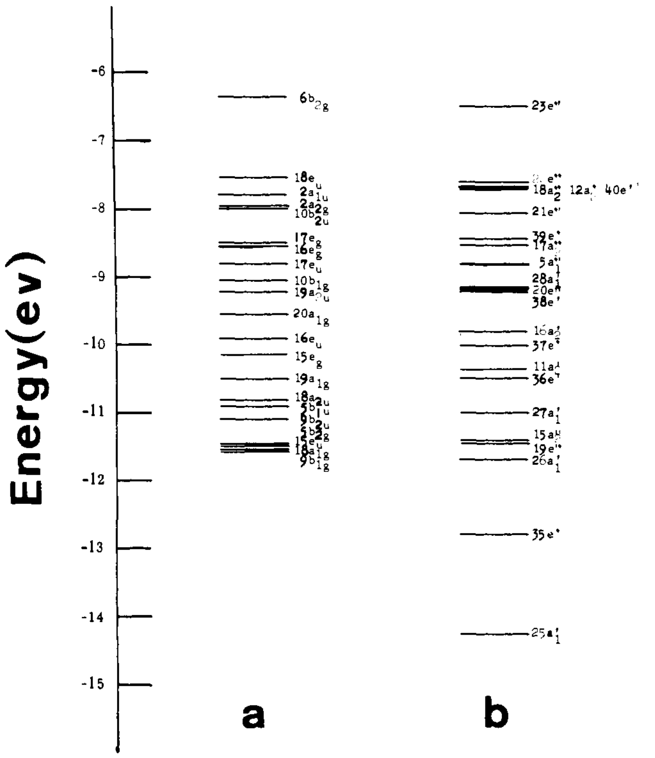

Figure 3. Valence orbital energy diagrams for (a) $Re_2Cl_8^{2-}$ and (b) Re_3Cl_9. Eigenvalues for $Re_2Cl_8^{2-}$ have been shifted so that the shallow metal core levels for the two calculations coincide.

-19.90 eV, account for 95% of Cl 3s character. The slightly greater s hybridization of chlorine in Re_3Cl_9 manifests itself in (1) greater splitting of the Cl s-like orbitals and (2) significant mixing into the higher 35e′, $26a_1'$, $27a_1'$, 36e′, and 40e′ valence levels.

An energy level diagram of the metal 5d and chlorine 3p based valence orbitals in $Re_2Cl_8^{2-}$ and Re_3Cl_9 may be found in Figure 3. In order to discuss the bonding we note that our choice of coordinate system in $Re_2Cl_8^{2-}$ takes the z direction on each atom to lie along the direction defined by the metal-metal vector. The chlorine atoms were taken to lie in the xz and yz planes. This choice of axis allows an approximate separation of Re–Cl interactions into σ and π components because of the approximate orthogonality of the Re–Re and Re–Cl vectors ($\angle$Re–Re–Cl = 103.7°).[13] Next, we classify the valence chlorine p levels according to the irreducible representations which they span. One set of orbitals (p_z) is oriented parallel to the metal-metal axis and forms a representation which can be decomposed into $a_{1g} + b_{1g} + e_g + a_{2u} + b_{2u} + e_u$. Because these orbitals can interact with Re in a chiefly π sense, we denote them $p\pi_\parallel$. The set of p orbitals on each center which primarily interact with the metal in a σ sense are denoted $p\sigma$ and span the same representation as $p\pi_\parallel$. There remains a set of chlorine p orbitals which are oriented perpendicular to the z direction and interact with Re in a π sense. These orbitals we denote $p\pi_\perp$ and they span a symmetry representation which can be reduced to the sum of $a_{2g} + b_{2g} + e_g + a_{1u} + b_{1u} + e_u$. Because the Re σ, π, δ, δ^*, π^*, $d_{x^2-y^2}$, $d_{x^2-y^2}$, σ^* orbitals span the respective representations a_{1g}, e_u, b_{2g}, b_{1u}, e_g, b_{1g}, b_{2u}, and a_{2u}, we note that $p\pi_\perp$ orbitals of a_{2g} and a_{1u} symmetry cannot interact with the metal. Consequently, the $2a_{2g}$ and $2a_{1u}$ orbitals are composed of nearly pure Cl 3p functions. These levels might be regarded as the "ideal lone pair" and levels lying below these are stabilized due to Re–Cl bonding.

Next systematically consider the interactions among both metal and ligand orbitals of a_{1g}, e_u, b_{2g}, b_{1u}, e_g, b_{1g}, b_{2u}, and a_{2u} symmetry. There are only three occupied a_{1g} orbitals (18–20 a_{1g}) derived from Re dσ, Cl pσ, and Cl $p\pi_\parallel$. Of these three levels 20 a_{1g} is the simplest, consisting of an equal admixture of Re dσ and Cl $p\pi_\parallel$ in an antibonding fashion. The 18 and $19a_{1g}$ orbitals are comprised of a complex admixture of all three components. Interactions among the occupied e_u levels are sensibly divided. Widely split 15 and $18e_u$ are in agreement with the earlier conclusion[15,16] that the Re dπ orbitals can interact with the Cl pσ orbitals in a bonding and antibonding sense; however, we find considerable (20%) and nearly equal Cl $p\pi_\parallel$ character in these orbitals which proves that metal-ligand π interaction may also contribute to the splitting. In valence bond terminology, the Cl $p\pi_\parallel$–pσ hybrid better points toward the metal d_{xz}, d_{yz} orbitals than would one directed approximately along the Re–Cl bond. Closely spaced 16 and $17e_u$ orbitals are primarily noninteracting "lone-pair" chlorine orbitals.

There are only two occupied b_{2g} orbitals. A bonding interaction between the Cl $p\pi_\perp$ orbitals of this symmetry and the Re dδ orbital yields $5b_{2g}$, a primarily halogen orbital. The antibonding counterpart $6b_{2g}$ is more familiarly called the metal-metal δ bonding orbital. The only occupied b_{1u} orbital at -10.89 derives from a Cl-$p\pi_\perp$ orbital (80%) stabilized by some π donation into the unoccupied rhenium dδ^* orbital. Weak stabilization of chloride lone pair orbitals may be found in the $16e_g$ orbital a Cl-$p\pi_\parallel$ to Re dπ^* donation. Little mixing occurs in $17e_g$, a chiefly Cl-$p\pi_\parallel$ type orbital. The 15 e_g orbital primarily consists of Cl pσ donation into one lobe of the Re dπ^* type orbital.

The b_{1g} and b_{2u} symmetry Re 5d orbitals are derived from the $d_{x^2-y^2}$ orbitals which point directly at the chloride ions. Accordingly, the occupied $9b_{1g}$ and $9b_{2u}$ orbitals are among the deepest valence band orbitals. These are comprised of Cl pσ character with substantial (30%) Re 5d character characteristic of a strong covalent bonding interaction, with considerable charge donation into the empty $d_{x^2-y^2}$ orbitals of rhenium. The higher lying $10b_{1g}$ and $10b_{2u}$ orbitals are lone-pair chlorine orbitals derived from $p\pi_\parallel$ and cannot interact with the $d_{x^2-y^2}$ orbitals because of the near-zero overlap.

Finally, the 18 and $19a_{2u}$ orbitals are chlorine based pσ and $p\pi_\parallel$ orbitals, respectively. The former is considerably stabilized owing to σ donation to the empty Re–Re σ^* orbital. Overlap between Cl-$p\pi_\parallel$ and d_{z^2} is expected to be small and the stabilizing interaction is expected to be much less in this case, as in $19a_{2u}$.

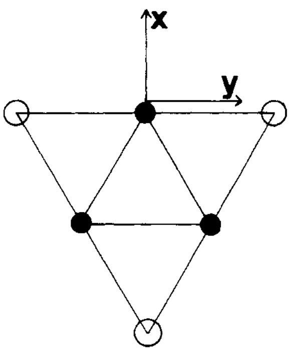

Figure 4. Choice of coordinate system for the Re_3Cl_9 calculation.

An analysis of the valence orbitals similar to that performed above for $Re_2Cl_8^{2-}$ proves more difficult for Re_3Cl_9, which possesses threefold symmetry. Figure 4 depicts our choice of coordinate system which defines the atomic basis orbitals for the topmost Re atom. The chief advantages of this choice are the separation of in-plane (X, Y) and out-of-plane (Z) interactions as well as the utility of this coordinate system for considering Re–Cl_b interactions. Fortunately, the Re–Re–Cl_b angle[12] (58.8°) results in Cl_b lying only 1° off the Y direction

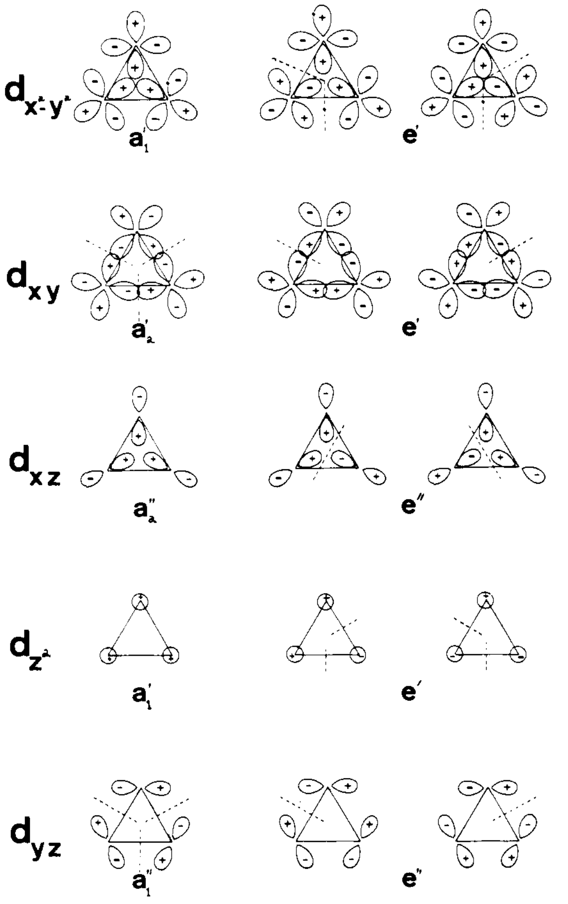

Figure 5. Symmetry-adapted combinations of the metal d orbitals in Re_3Cl_9.

of the Re-centered coordinate system. The coordinate systems chosen for the terminal (not shown) and bridging chloride ions attached to the designated Re atom were assumed parallel to the Re coordinates. Symmetry combinations of the Re 5d valence orbitals span the irreducible representations $2a_1' + a_2' + 3e' + a_1'' + a_2'' + 2e''$ and these are depicted in Figure 5. The p_x orbitals of terminal chlorine span $a_1' + a_2'' + e' + e''$ representations, as also do the p_z orbitals. Terminal chlorine p_y orbitals comprise $a_2' + a_1'' + e' + e''$ symmetry species. Bridging chlorine p_x and p_z orbitals span $a_1' + a_2' + 2e'$ irreducible representations and the p_z orbitals comprise $a_2'' + e''$ symmetry representations.

As in $Re_2Cl_8{}^{2-}$ some primarily chlorine-based "lone pair" orbitals $11a_2'$, $37e'$, $28a_1'$, $40e'$, $12a_2'$, and $22e''$ are found between −10.4 and −7.6 eV. Only two levels, $25a_1'$ and $15a_2''$, consist of mainly Re 5d. Interestingly enough, these correspond (70% contribution) to the cluster $d\sigma$ and $d\pi$ bonds formed from the a_1' ($d_{x^2-y^2}$) and a_2'' (d_{xz}) symmetry combinations of Figure 5. The $25a_1'$ level is particularly unique since considerable Re 6s and $5p_x$ character are mixed into the orbital wave function, while the chlorine atomic orbital contributions total less than 4%. This hybridization tends to maximize the directionality of the three-center σ-bonding orbital toward the cluster center. The strength of this interaction is truly remarkable, as evidenced by the low energy of this orbital. The $15a_2''$ three-center $d\pi$ bonding ($d_{xz}a_2''$, Figure 5) orbital is quite stable, but mixes in a significant terminal chlorine p contribution which can interact with the Re d_{xz} orbitals in a π manner. Level $18a_2''$ exhibits the antibonding π interaction with the terminal chlorine.

Some appreciable Cl–Cl interactions also appear to occur. Levels $16a_2''$ and $17a_2''$ are noticeably split and appear to be bonding and antibonding counterparts of bridging chlorine–terminal chlorine overlap. Equally confusing is the exact nature of the $39e'$ and $21e''$ halide orbitals.

The remaining valence orbitals exhibit covalent metal–ligand interactions. One might have thought that the e' combination of the metal d_{xy} orbitals (Figure 5) would correspond to Re–Re single bonds along the edges of the triangle. While the $35e'$ level does consist of considerable metal d_{xy} character, the p_x and p_y orbitals of the bridging chlorines contribute to an equal extent. Rather than being described as a metal–metal bond it is more proper to qualitatively regard this orbital as a three-center σ-bonding orbital (Re–Cl_b–Re σ). Its approximately nonbonding counterpart $38e'$ is also occupied.

Donation, in a σ sense, of chlorine p_x–p_y–s hybrid orbitals into the a_1' combination of Re d_{z^2} (Figure 5) occurs in $26a_1'$. Noteworthy is the fact that no single orbital contains dominant Re d_{z^2} character, but that its contribution to the bonding orbitals is spread over the $25a_1'$ (12%), $35e'$ (7%), $26a_1'$ (18%), $27a_1'$ (14%), and $36e'$ (21%) levels.

The e'' combination of the metal d_{yz} orbitals (Figure 5) is expected to result in small metal–metal overlap, but is oriented properly to π bond with both bridging and terminal chlorides. Bonding character of precisely this type is found in $19e''$, and $23e''$ is the related antibonding partner. Antibonding character of the latter highest occupied molecular orbital is further evidenced by the small (<0.5 eV) half-width of the first band in the photoelectron spectrum (Figure 2). Further Re d_{yz}–Cl(terminal) interaction occurs in the $5a_1''$ orbital, which can be described as π donation from terminal chlorine p(a_1'') into the Re d_{z^2} orbital combination of this symmetry (Figure 5). σ bonding between p or sp hybrids of the terminal chlorines with a_1' and e' combinations of the Re d_{z^2} orbitals may be found in the occupied $27a_1'$ and $36e'$ orbitals. Finally, the $20e''$ level results from weak σ mixing between a terminal chlorine p_z and p_x hybrid with the e'' combination of d_{yz}.

Several important differences may be noted when comparing the electronic structures of $Re_2Cl_8{}^{2-}$ and Re_3Cl_9. A glance at Figure 3 reveals that the splitting of valence levels in Re_3Cl_9 is considerably greater than in $Re_2Cl_8{}^{2-}$ and owes to the great stability of the $25a_1'$, $35e'$, $19e''$, and $15a_2''$ bonding levels. Appropriately, these orbitals reflect the special bonding properties of the trinuclear cluster complex. Most of the significant metal–metal bonding interactions in Re_3Cl_9 result from the three-center metal σ and π overlap found in the $25a_1'$ and $15a_2''$ orbitals. Delocalized rhenium chlorine σ and π bonding (vide supra) are found in $35e'$ and $19e''$, respectively. In both levels appreciable three-center Re–Cl_b–Re interactions are evident.

A qualitative picture of metal–metal interactions among three Re(III) ions (assuming equilateral triangular geometry) was given by Cotton and Haas[22] some years ago. Adopting their convention that the z axis on every rhenium atom directs toward the triangle center and taking the x axis of the right-handed coordinate system in the plane, they predicted the bonding level ordering to be $e''(xy) > e'(xz) > a_2''(yz) > a_1'(z^2)$. These correspond to the respective orbitals $23e''$, 35 and $38e'$, $15a_2''$, and $25a_1'$ in the present calculation. The deep $25a_1'$ and $15a_2''$ valence orbitals do closely approximate metal-localized orbitals which contribute to strong metal-metal bonding; however, the 35 and $38e'$ and $23e''$ levels contain substantial character of both terminal and bridging halide and should not be ascribed to simple metal–metal bonding. Qualitatively, the metal interaction model provides a useful theoretical framework for the more complex analysis given above.

Recently Cotton and Stanley[23] published preliminary details of a SCF Xα SW or overlapping spheres calculation for Re_3Cl_9. Both their and our calculations agree that the highest occupied orbital is $23e''$ (note that their designation is $6e''$).

Also, the 1-eV gap to the second IP is predicted by both procedures; however, there are minor (±0.3 eV) differences. For example, we find the second occupied orbital to be $22e''$ whereas the alternative calculation method predicts that $5a_2''$ and $2a_2'$ are occupied before $22e''$.

Perhaps the most interesting distinctions occur in the charge density analysis. To contrast the percent metal character in the orbitals attributable to metal–metal bonding compare (% Re this work–% Re ref 23): $23e''$ (50–63), $18a_2''$ (27–45), $38e'$ (62–74), $27a_1'$ (16–58), $15a_2''$ (72–59), $26a_1'$ (22–70), $35e'$ (44–52), $25a_1'$ (95–43). The two calculations differ markedly as to how the metal–metal interactions are divided among the occupied a_1' orbitals. At the present time the origin of these varying descriptions is not clear. Possible influences include the difference between the muffin tin and the s wave expanded potential as well as the problem of appropriating extrasphere charge in the overlapping spheres procedure. Our procedure suffers from the usual deficiencies of a Mulliken-type analysis. Further study will be necessary to clarify this point.

Conclusions

An insufficient body of experimental–theoretical data exists for trinuclear metal cluster complexes to allow a comparison with other systems. We can, though, comment on the connection between the ground-state electronic structure of rhenium(III) chloride complexes and their chemical properties. Covalent Re–Cl bonding found in Re_3Cl_9 chemically manifests itself in the robust nature of the Re_3Cl_9 moiety. Complexes of the type $Re_3Cl_9L_3$[4,12,24] (L = Cl, Br, PR_3, OSR_2, NC_5H_5, OPR_3) have been synthesized by adding L to solid Re_3Cl_9 or to solutions in coordinating solvents. In all cases L binds terminally to Re in the plane of the Re_3 triangle. No instances have been reported where any of the nine chlorine atoms can be simply substituted under mild conditions.

Another relevant observation pertains to the in-plane trans effect found in $Re_3Cl_9L_3$ complexes. Recall that both structural and chemical evidence[12] shows that the three ligands, L, are bound weakly in the plane of the Re_3 triangle. This parallels a trend found in binuclear Mo(II), Re(III), and Cr(II) complexes. These compounds which adopt D_{4h} M_2L_8 structures are capable of weakly binding two axial ligands.[25] It has been well established[25] that the tendency to bind axial ligands diminishes as the metal–metal bond strengthens. Cotton[25] likened this to a trans effect of the metal–metal bond. We propose that the Re_3Cl_9 trinuclear cluster complex derivatives provide examples of a *cluster bonding trans effect.* The $25a_1'$ orbital is the deepest occupied metal–metal bonding orbital. One therefore might reasonably assume that the most significant bonding metal–metal interactions occur in this level. This orbital corresponds chiefly to the σ bonding combination of d orbitals which mix in significant metal s and p character in order to point toward the center of the triangle. Because these orbitals are so strongly metal–metal bonding, no suitable σ-acceptor orbital exists for the ligands, L, in the $Re_3Cl_9L_3$ complexes, a feature entirely analogous to axial ligand binding in the M_2L_8 complexes. Studies are in progress to determine whether the in-plane trans effect is a general feature of trinuclear metal cluster complexes, since only seldom are ligands found at the vertices of trinuclear metal cluster complexes.

Acknowledgments. We thank Dr. Charles Batson for assistance with spectral plots and Dr. S. T. Manson for communication of some results prior to publication. Professor F. A. Cotton and Mr. George Stanley are thanked for helpful suggestions. W.C.T. acknowledges the Research Corporation and the Northwestern University Research Committee for support of this work. He also thanks the Argonne Center for Educational Affairs and the Physics Division of ANL for a Guest Faculty Research Participation appointment. D.E.E. acknowledges support of the National Science Foundation, Grant DMR77-22646, and use of facilities of the Northwestern University Materials Research Center. Work performed at ANL was done under the auspices of the Division of Basic Energy Sciences of the U.S. Department of Energy.

References and Notes

(1) (a) Northwestern University. (b) Argonne National Laboratory.

(2) (a) Muetterties, E. L. *Bull. Soc. Chim. Belg.* **1975,** *84,* 959. *Angew. Chem. Int. Ed. Engl.* **1978,** *17,* 545. Chini, P.; Longoni, G.; Albano, V. G. *Adv. Organomet. Chem.* **1976,** *14,* 285. (b) Laine, R. M.; Rinker, R. G.; Ford, P. C. *J. Am. Chem. Soc.* **1977,** *99,* 252. Thomas, M. G.; Beier, B. F.; Muetterties, E. L. *Ibid.* **1976,** *98,* 1296. Deeming, A. J.; Hasso, S. *J. Organomet. Chem.* **1976,** *114,* 313. Sanchez-Delgado, R. A.; Bradley, J. S.; Wilkinson, G. *J. Chem. Soc., Dalton Trans.* **1976,** 399. Braca, G.; Sbrana, G.; Piacenti, F.; Pino, P. *Chim. Ind.* (*Milan*) **1970,** *52,* 1091. Casey, C. P.; Cyr, C. R. *J. Am. Chem. Soc.* **1973,** *95,* 2248. Bingham, D.; Hudson, B.; Webster, D. E.; Wells, P. B. *J. Chem. Soc., Dalton Trans.* **1974,** 1521, Castiglioni, M.; Milone, D.; Osella, D.; Vaglio, G. A.; Valle, M. *Inorg. Chem.* **1976,** *15,* 394. Pregaglio, G.; Andreelta, A.; Ferrari, G.; Ugo, R. *J. Organomet. Chem.* **1971,** *33,* 73. Eplattenier, F. L.; Matthys, P.; Calderazzo, F. *Inorg. Chem.* **1970,** *9,* 342.

(3) Norman, J. G.; Kolari, H. J. *J. Am. Chem. Soc.* **1978,** *100,* 791. Trogler, W. C.; Gray, H. B. *Acc. Chem. Res.* **1978,** *11,* 232. Cotton, F. A. *Ibid.* **1978,** *11,* 225. Martin, D. S.; Newman, R. A.; Fanwick, P. E. *Inorg. Chem.*, in press. Wrighton, M. S. *Top. Curr. Chem.* **1976,** *65,* 37. Dubicki, L.; Martin, R. L. *Aust. J. Chem.* **1969,** *22,* 1571. Dedieu, A.; Hoffmann, R. *J. Am. Chem. Soc.* **1978,** *100,* 2074. Sattelberger, A. P.; Fackler, J. P. *Ibid.* **1977,** *99,* 3620. Garner, D. C.; Hillier, I. H.; Guest, M. F.; Green, J. C.; Coleman, A. W. *Chem. Phys. Lett.* **1976,** *41,* 91. Clark, R. J. H.; D'Urso, N. R. *J. Am. Chem. Soc.* **1978,** *100,* 3088. Buchanan, R. M.; Kessel, S. L.; Downs, H. H.; Pierpont, C. G.; Hendrickson, D. N. *Ibid.* **1978,** *100,* 7894. References contained in the above articles.

(4) Cotton, F. A.; Mague, J. T. *Inorg. Chem.* **1964,** *3,* 1402.

(5) Howard, W. F.; Andrews, L. *Inorg. Chem.* **1975,** *14,* 1726.

(6) Berkowitz, J. *J. Chem. Phys.* **1972,** *56,* 1766.

(7) Newburgh, R. G.; Heroux, L.; Hinteregger, H. E. *Appl. Opt.* **1962,** *1,* 733. Newburgh, R. G. *Ibid.* **1963,** *2,* 864.

(8) Moore, C. E. "Atomic Energy Levels", *Natl. Bur. Stand.* (*U.S.*), *Circ.* **1958,** 467.

(9) Büchler, A.; Blackburn, P. E.; Stauffer, J. L. *J. Phys. Chem.* **1966,** *70,* 685. Nikolaev, E. M.; Ovchinnikov, K. V.; Semenov, G. A. *Zh. Obshch. Khim.* **1970,** *40,* 1302. Mamyrin, B. A.; Karataev, V. I.; Shmikk, D. V.; Zagulin, V. A. *Zh. Eksp. Teor. Fiz.* **1973,** *64,* 82.

(10) Averill, F. W.; Ellis, D. E. *J. Chem. Phys.* **1973,** *59,* 6412. Rosen, A.; Ellis, D. E. *Ibid.* **1976,** *65,* 3629, and references cited therein.

(11) Trogler, W. C.; Ellis, D. E., unpublished results.

(12) Bertrand, J. A.; Cotton, F. A.; Dollase, W. A. *Inorg. Chem.* **1963,** *2,* 1166. Fergusson, J. E. *Prep. Inorg. React.* **1971,** *7,* 93, and references cited therein.

(13) Cotton, F. A.; Harris, C. B. *Inorg. Chem.* **1967,** *6,* 924.

(14) Dubicki, L.; Martin, R. L. *Aust. J. Chem.* **1969,** *22,* 1571.

(15) Mortola, A. P.; Moskowitz, J. W.; Rösch, N. *Int. J. Quantum. Chem., Symp.* **1974,** *No. 8,* 161.

(16) Norman, J. G.; Kolari, H. J. *J. Am. Chem. Soc.* **1975,** *97,* 33.

(17) This work.

(18) Bernard, M.; Veillard, A.; *Nouveau J. Chim.* **1977,** *1,* 97.

(19) Hay, P. J. *J. Am. Chem. Soc.* **1978,** *100,* 2897.

(20) King, G. H.; Krishanamurty, S. S.; Lappert, M. F.; Pedley, J. B. *Discuss. Faraday Soc.* **1973,** *54,* 70. Wittel, K.; Manne, R. *J. Chem. Phys.* **1975,** *63,* 1322. Manne, R.; Wittel, K.; Mohanty, B. S. *Mol. Phys.* **1975,** *29,* 485.

(21) McGuire, E. J. "Atomic Subshell Photoionization Cross Sections for $2 < Z < 54$, Sandia Laboratories Report SC-RR-70-721, 1970. Mason, S. T.; Starace, A. F.; Shahabi, S. *Phys. Rev. A,* submitted. Manson, S. T., private communication, 1979.

(22) Cotton, F. A.; Haas, T. E. *Inorg. Chem.* **1964,** *3,* 10.

(23) Cotton, F. A.; Stanley, G. G. *Chem. Phys. Lett.* **1978,** *58,* 450.

(24) Fergusson, J. E.; Penfold, B. R.; Robinson, W. T. *Nature* (*London*) **1964,** *201,* 181. Elder, M.; Penfold, B. R. *Ibid.* **1965,** *205,* 276. Cotton, F. A.; Mague, J. T. *Inorg. Chem.* **1964,** *3,* 1094. Cotton, F. A.; Lippard, S. J.; Mague, J. T. *Ibid.* **1965,** *4,* 508. Tisley, D. G.; Walton, R. A. *Ibid.* **1973,** *12,* 373.

(25) Collins, D. M.; Cotton, F. A.; Murillo, C. A. *Inorg. Chem.* **1976,** *15,* 1861.